



# Intracranial MEMS based temozolomide delivery in a 9L rat gliosarcoma model

Byron C. Masi<sup>a,b</sup>, Betty M. Tyler<sup>c</sup>, Hansen Bow<sup>c</sup>, Robert T. Wicks<sup>c</sup>, Yuan Xue<sup>b</sup>, Henry Brem<sup>c,d,e</sup>, Robert Langer<sup>a,b</sup>, Michael J. Cima<sup>b,f,\*</sup>

<sup>a</sup> Department of Chemical Engineering, Massachusetts Institute of Technology, Cambridge, MA 02139, USA

<sup>b</sup> The David H. Koch Institute for Integrative Cancer Research, Massachusetts Institute of Technology, Cambridge, MA 02139, USA

<sup>c</sup> Department of Neurosurgery, Johns Hopkins University School of Medicine, Baltimore, MD 21231, USA

<sup>d</sup> Department of Oncology, Johns Hopkins University School of Medicine, Baltimore, MD 21231, USA

<sup>e</sup> Department of Biomedical Engineering, Johns Hopkins University School of Medicine, Baltimore, MD 21231, USA

<sup>f</sup> Department of Materials Science & Engineering, Massachusetts Institute of Technology, Cambridge, MA 02139, USA

## ARTICLE INFO

### Article history:

Received 11 April 2012

Accepted 21 April 2012

Available online 14 May 2012

### Keywords:

MEMS

Glioma

Microchip

Temozolomide

Drug delivery

Localized delivery

## ABSTRACT

Primary malignant brain tumors (BT) are the most common and aggressive malignant brain tumor. Treatment of BTs is a daunting task with median survival just at 21 months. Methods of localized delivery have achieved success in treating BT by circumventing the blood brain barrier and achieving high concentrations of therapeutic within the tumor. The capabilities of localized delivery can be enhanced by utilizing micro-electro-mechanical systems (MEMS) technology to deliver drugs with precise temporal control over release kinetics. An intracranial MEMS based device was developed to deliver the clinically utilized chemotherapeutic temozolomide (TMZ) in a rodent glioma model. The device is a liquid crystalline polymer reservoir, capped by a MEMS microchip. The microchip contains three nitride membranes that can be independently ruptured at any point during or after implantation. The kinetics of TMZ release were validated and quantified *in vitro*. The safety of implanting the device intracranially was confirmed with preliminary *in vivo* studies. The impact of TMZ release kinetics was investigated by conducting *in vivo* studies that compared the effects of drug release rates and timing on animal survival. TMZ delivered from the device was effective at prolonging animal survival in a 9L rodent glioma model. Immunohistological analysis confirmed that TMZ was released in a viable, cytotoxic form. The results from the *in vivo* efficacy studies indicate that early, rapid delivery of TMZ from the device results in the most prolonged animal survival. The ability to actively control the rate and timing of drug(s) release holds tremendous potential for the treatment of BTs and related diseases.

© 2012 Elsevier Ltd. All rights reserved.

## 1. Introduction

Brain cancer only accounts for 1.4% of all cancer diagnoses and 2.3% of all cancer deaths (American Cancer Society, Cancer Facts, 2011), yet it remains one of the most intimidating and challenging cancers to treat. The most common and aggressive form of adult malignant brain tumor is glioblastoma multiforme (GBM) [1], and despite the best treatment, the median survival of people diagnosed with this disease is just 21 months [2].

Treatment generally involves a combination of surgical resection, radiotherapy, and chemotherapy [3]. Chemotherapy is conventionally administered systemically via intravenous injection or oral formulations. Current BT therapy is largely based around the Stupp protocol, a combination of radiotherapy with oral

administration of the alkylating agent temozolomide (TMZ). This combination has been shown to increase median survival from 12 months with radiotherapy alone to approximately 15 months with combined radiotherapy and oral TMZ [4]. One of the major limitations to the development of more effective brain tumor therapies is the presence of the blood–brain barrier, which prohibits the transfer of molecules that are larger than 500 Da or are non lipid-soluble [5]. Unfortunately, most chemotherapeutics do not fit these criteria; systemic toxicity is often reached before obtaining a therapeutically effective concentration in the brain when the delivery method is either intravenous or oral.

Various localized delivery methods, such as convection enhanced delivery or locally implanted drug depots, have therefore been studied as an alternative mechanism of drug delivery to the brain [6–15]. One successful method has been the implantation of a biodegradable, drug-eluting polymer wafer during surgical resection of the tumor. The drug delivery system, Gliadel<sup>®</sup>, is based on this technology and provides for the controlled release of the

\* Corresponding author. The David H. Koch Institute for Integrative Cancer Research, Massachusetts Institute of Technology, Cambridge, MA 02139, USA  
E-mail addresses: [mjcima@mit.edu](mailto:mjcima@mit.edu), [M.J.Cima@mjcima@mit.edu](mailto:M.J.Cima@mjcima@mit.edu) (M.J. Cima).

alkylating agent carmustine [16,17]. Implantation of these wafers during tumor resection surgery increases median survival 2–4 months for patients with recurrent glioblastoma [18]. In combination with the systemic chemotherapy temozolomide and radiation these implants have increased median survival from 9 to 20 months [2]. Once Gliadel is implanted, however, the drug identity, quantity, and delivery rate cannot be changed without further intervention. Other passive delivery methods, such as locally implanted polymers, and passive drug depots, also suffer from these limitations [19,20].

The versatility in function of drug depots, such as Gliadel®, can be enhanced by utilizing micro-electro-mechanical system (MEMS) technology. MEMS based devices offer the exquisite advantage of being able to actively control the function of a device via minute electrical signals. Such communication offers the ability to control drug release rate and when drug release begins, allowing for the creation of complex temporal profiles of single or multiple therapeutics [21–28]. Controlled release devices utilizing MEMS technology have been used for *in vivo* delivery of small molecules and polypeptides and have demonstrated efficacy in reducing tumor progression in a rodent flank gliosarcoma model [22,23,29–31]. The first human trials, in fact, with a microchip drug delivery device were just completed with stunning success [32]. These devices, however, have previously been restricted to implantation in the subcutaneous space due to prohibitively large structural components.

We introduce a MEMS based intracranial drug delivery device to overcome the limitations of passive intracranial drug delivery systems. This device involves 3 membranes covering holes in a silicon microchip, which caps a reservoir containing drug. Each of these 3 membranes can be independently opened, or ‘activated’, by applying a short electrical pulse, thus allowing for active control over drug release rate. Activation, furthermore, can occur at any point during or after implantation. We first evaluated the kinetics of drug release *in vitro* and the potential toxicity and possible adverse effects of the device’s intracranial presence *in vivo*. We then evaluated the efficacy of drug release kinetics in treating a 9L rat glioma model with the chemotherapy drug temozolomide in the reservoir. We conclude with comparing the efficacy of this method of drug delivery with a polymer-based TMZ drug delivery system.

## 2. Materials & methods

### 2.1. Chemicals

Temozolomide was generously provided by the Developmental Therapeutics Program at the National Institute of Health. HPLC grade water, acetonitrile, ammonium acetate and polyethylene glycol were purchased from Sigma–Aldrich.

### 2.2. Device components

300  $\mu\text{m}$  thick silicon nitride coated silicon wafers were purchased from Silicon Quest Intl (San Jose, CA). Liquid crystalline polymer (LCP) reservoirs were purchased from MicroPEP (East Providence, RI). Flexible printed circuits boards (leads) were purchased from Flexible Circuit Technologies (Minneapolis, MN). Biomedical grade UV epoxy was purchased from Dymax Corp. (Torrington, CT). Biomedical grade cyanoacrylate was purchased from Loctite.

### 2.3. TMZ analytics

The HPLC method was adapted from Kim et al., 1997 [33]. Briefly, 20  $\mu\text{L}$  of sample was quantified at 10 °C on an Agilent 1200 Series HPLC using a Synchropak SCD-100, 5  $\mu\text{m}$ , 150  $\times$  4.6 mm column (Synchro, Lafayette, IN, USA), a flow-rate of 1 ml/min, 0.01 M ammonium acetate (aq):acetonitrile (92:8) mobile phase, and UV absorption at 316 nm.

### 2.4. Microchip fabrication

The fabrication process for the microchip portion of the active device has been described previously [34]. Briefly, one side of the wafer was patterned via standard photolithography and etched via reactive ion etching (RIE) to define  $\sim 720 \mu\text{m}$  by 720  $\mu\text{m}$  regions of bare silicon. Exposure to 20% KOH solution resulted in a self-terminating etch that created 300 by 300  $\mu\text{m}$  suspended  $\text{Si}_3\text{N}_4$  membranes. Titanium (30 nm) and gold (250 nm) layers were sputtered onto the same side of the wafer as the nitride membranes. Thin (40  $\mu\text{m}$ ) metallic ‘fuses’ were then defined using standard photolithography, followed by wet etching steps using gold and titanium etchants. All MEMS microfabrication processes were carried out at the Microsystems Technology Laboratories of MIT.

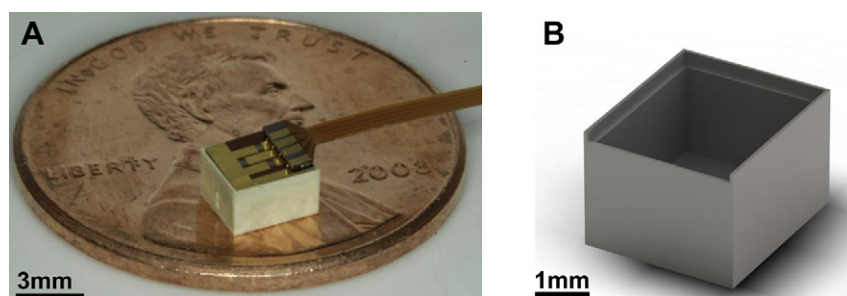
### 2.5. Reservoir design and fabrication

Fig. 1B is digital rendering of the device reservoir. The reservoir is injection molded out of liquid crystalline polymer (LCP, Vectra 1300) by microPEP (East Providence, RI). The inner dimensions of the reservoir were sized such that it would contain a 10 mg payload of TMZ when loaded in powder form and could be capped by a 3 membrane chip. The overall reservoir dimensions are 3.7 by 3.2 by 2.2 mm. The side and bottom walls are 400  $\mu\text{m}$  thick. A 200  $\mu\text{m}$  wide shelf was designed into the inner wall of the reservoir. This shelf and the bordering walls serve as a seat for the chip, ensuring reproducible alignment and sealing between the chip and reservoir. The shelf is recessed 400  $\mu\text{m}$  from the top of the reservoir such that when the 300  $\mu\text{m}$  thick chip is placed in the reservoir and rests on the shoulder, a thin bead of epoxy can be run around the perimeter of the chip thus securing the chip and isolating the contents of the reservoir from the environment (Fig. 1A).

### 2.6. Device filling

Reservoirs were loaded with TMZ in solid form in order to maximize payload and drug stability [35]. Polyethylene glycol (PEG) was added to displace air trapped within the packed TMZ powder, therefore reducing air bubble formation within the reservoir. Molecular weight 1450 PEG was used because its melting temperature is between 43 and 46 °C. The PEG, therefore, is solid when implanted at body temperature, but the TMZ:PEG mixture can be melted at moderate temperatures [35].

The process begins by packing the reservoir with TMZ powder. The reservoir is then placed in a fixture that allows molten PEG to be pipetted onto the TMZ in each reservoir. The second half of the fixture is then joined with the first half such that a high air permeability Teflon AF membrane (Biogeneral Inc, San Diego, CA) is fixed



**Fig. 1.** Color photograph of the device (A) and a CAD render of the LCP reservoir (B). Photograph of the fully assembled device. The white LCP reservoir is capped by the purple and gold microchip. The 3 green squares on the microchip are the suspended nitride membranes. The polyimide coated copper leads protrude from the device (A). The reservoir dimensions are 3.7 by 3.2  $\times$  2.2 mm. The total drug payload is 10 mg of TMZ. The 200  $\mu\text{m}$  shelf is visible on the interior face of the reservoir walls. This shelf serves as a seat for the chip and as an upper boundary for drug during the loading process. A lead-way was designed in the top perimeter of the chip to allow the polyimide leads to project out from the device (B).

over the PEG:TMZ surface. The assembled fixture is placed in a vacuum oven and vacuum is pulled at 55 °C for 20 min. When the two halves of the fixture are joined the only path for air to travel is through the membrane and out of the fixture. The TMZ and PEG are therefore trapped within the reservoir, but air is free to flux out. Under vacuum and 55 °C conditions, the air within the powder drug fluxes out of the reservoir through the Teflon membrane. The molten PEG is then free to wet the TMZ powder and fill in the interstices of the packed TMZ, therefore creating a homogeneous mixture of TMZ and PEG throughout the reservoir. This process is repeated (typically 3 times) until all of the air has been removed from the PEG:TMZ mixture.

### 2.7. Device assembly

Polyimide coated copper leads were attached to each chip by biomedical grade cyanoacrylate. Each copper lead was gold wire bonded to its corresponding gold pad on the chip thus achieving electrical connectivity (Fig. 1A).

The chip:lead assembly was then placed on the shoulder structure of the reservoir such that the upper most walls of the reservoir surround the chip. A bead of biomedical grade UV curable epoxy is then run around the perimeter of the chip such that it fills the gap between chip and reservoir wall. The epoxy was then cured in place with a compatible UV light source.

### 2.8. Release procedures

TMZ devices were filled with known amounts of drug and then activated and placed in stirred baths at 37 °C. Release studies were conducted in water. The bath volume and frequency of sampling was varied to ensure that samples contained quantifiable amounts of drug, but maintained approximate sink conditions. Release bath samples were acidified to pH 1 with HCl to prevent degradation during analysis. Samples were analyzed for TMZ content via the HPLC method described above.

### 2.9. Animal implantation protocol

Female Fisher 344 rats weighing 125–175 g were purchased from Charles River Laboratories (Wilmington, DE). All animals were given free access to food and water at all times. All animals were housed in accordance with the Johns Hopkins University Care and Use Committee rules and regulations. Animals were intracranially implanted with 9L gliosarcoma obtained from the UCSF Tumor Bank (San Francisco, CA) that has been passaged continuously in carrier flanks of F344 rats.

The intracranial tumor and/or device implantation method used, as previously detailed by Brem et al. [12], is briefly described here. Animals were anesthetized with an intraperitoneal (i.p.) injection of 3–5 ml/kg of a stock solution containing ketamine hydrochloride 25 mg/ml (Ketlar; Parke-Davis Corporation Morris Plains, NJ), xylazine 2.5 mg/ml (Rompun; Mobay Corp., Shawnee, Kansas), and 14.25% ethyl alcohol in 0.9% NaCl. All surgical procedures were carried out using standard sterile surgical technique. The head was shaved and prepared with alcohol and prepodyne solution. A midline scalp incision was made, exposing the sagittal and coronal sutures. A small burr hole was drilled, centered 3 mm lateral to the sagittal suture (avoiding the sagittal sinus) and 5 mm posterior to the coronal suture. The 9L tumor and/or device was implanted and animals were then randomized into various treatment groups. The incision was then closed with staples and the animal allowed to recover.

#### 2.9.1. Biocompatibility study

All techniques described above were used in the biocompatibility study. The animals, however, received only implantation of the unactivated device (no tumor). This study involved 5 rats, and weight was used as a proxy for health. The rats were sacrificed on predetermined days 1, 2, 3, and 7 post-implantation and autopsies performed to determine whether the chips caused toxic side effects.

#### 2.9.2. Efficacy studies

A 9L tumor piece and the TMZ-filled device were implanted on day 0 and animals were assigned to various treatment groups. Devices were activated on the specified days (either day 0, 3 or 5) post-tumor implantation by anesthetizing the animal, removing the staples, locating the electrical leads, and applying a brief electrical pulse. The incision was then closed with staples and the animal allowed to recover. Polymer wafers were implanted on day 5 after anesthetizing the animal and removing the staples. The wafers were implanted through the burr hole, the incision was stapled closed and the animal was allowed to recover.

Animals were observed daily for behavior, gait, grooming, weight loss, and mobility. Animals were euthanized when they became moribund and the MEMS device was removed for analysis and the brain was placed in formalin or flash frozen for subsequent histological and immunohistochemical analysis.

### 2.10. Immunohistological analyses

Rat brain tissues were fixed with 4% paraformaldehyde at 4 °C overnight. Tissue samples were washed with phosphate-buffered saline (PBS), and then embedded in paraffin. Longitudinal brain sections of 5  $\mu$ m thickness were prepared for further immunohistological analyses. Tissue slides were stained as previously described [36]. Briefly, tissue slides were blocked with 3% goat serum in PBS for 30 min, and

were incubated with polyclonal rabbit anti-Caspase-3 (Abcam, UK, 1:200 dilution) or polyclonal anti-Ki67 (Abcam, UK, 1:200 dilution) antibodies at 4 °C overnight and then washed with PBS. A secondary anti-rabbit Alexa-488 (Invitrogen, US, 1:500 dilution) antibody was added onto the tissue sections and incubated for 45 min. Sections were washed with PBS, followed by counter-staining with DAPI. The stained samples were mounted with the Vectashield mounting medium (Vector Laboratories, US) and stored at 4 °C until further analyses. Images were captured with 20 $\times$  objective by Zeiss AxioPlan2 fluorescent microscopy. Three representative images were taken for each sample. Adobe Photoshop was used to quantify the positive signal.

## 3. Results

The device consists of a reservoir containing TMZ that is covered by a microchip containing 3 nitride membranes that can be independently opened by applying a brief (0.4 ms) electrical pulse. This electrical pulse causes resistive heating, which causes expansion of the gold fuse and rupture, 'activation', of the underlying nitride membrane [34]. The patency of each membrane can be assessed by monitoring the electrical resistance across the respective leads. Activation of a membrane allows the TMZ:PEG mixture to imbibe water, allowing TMZ to release into the surrounding tissue.

The *in vitro* release kinetics of opening various numbers of membranes in a single device was first quantified. The impact of implanting a device in the brain of a healthy rat was assessed by monitoring the health of that rat. The effect of whether a faster rate of drug delivery, as opposed to longer duration, resulted in better median survival was investigated. The impact of the timing of drug delivery on survival was evaluated. The microchip-based delivery method was compared to polymer-based delivery of TMZ. Histological analysis of tissue samples obtained from the efficacy study was conducted to confirm that TMZ retains its cytotoxic potential throughout the formulation, packaging and release process.

### 3.1. *In vitro* release studies

*In vitro* release studies were conducted to characterize the release kinetics of PEG co-formulated TMZ from the active device. These studies were conducted on groups of devices with either 3, 2, 1 or 0 membranes ruptured.

Fig. 2 is a plot of the release of TMZ into water as a function of time. Release curves are shown for devices ( $n = 3$ ) with 3, 2, 1 and zero membranes activated. Devices with zero membranes ruptured serve as controls to verify that TMZ release is dependent on device activation. These 'leak test' devices remained robustly sealed over the time scale required for the 3 and 2 membrane activated devices to release their payload, and an equivalent time scale for the 1 membrane activated devices to release their payload. The leak test devices ultimately began leaking after approximately 700 h (30 days) in 37 °C water.

The activated devices display reproducible release kinetics that vary with the number of membranes activated. Three membrane activated devices release with an average rate of 0.3 mg per hour (mg/h) achieving a final release of  $90 \pm 3.2\%$  in approximately 30 h. Two membrane activated devices release with an average rate of 0.136 mg/h, achieving a final release of  $82 \pm 1.9\%$  in about 60 h. One membrane activated devices release with a rate of 0.007 mg/h achieving an overall release of  $60 \pm 12\%$  over roughly 800 h ( $\sim 34$  days). This set of experiments verified and quantified our hypothesis that opening up more membranes results in faster drug release.

### 3.2. *In vivo* studies

#### 3.2.1. Impact of intracranial device implantation on animal health

The toxicity of implanting an unactivated microchip inside the brain of a rat was evaluated. This study involved 5 rats, and used

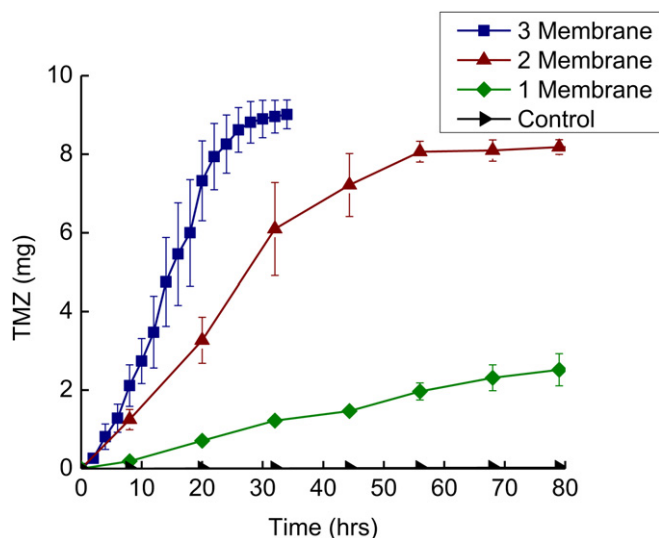


**Fig. 2.** Release curves for TMZ-filled devices releasing into 37 °C water. Devices ( $n = 3$ ) with 3, 2, 1 or 0 membranes activated were placed in stirred baths and sampled for TMZ content. The errors bars are the standard error. Release is a function of the number of activated membranes and release does not occur unless the device is activated.

weight as a proxy for health. The rats were sacrificed on pre-determined days 1, 2, 3, and 7 post-implantation and autopsies were performed to determine whether the chips caused toxic side effects. No gross abnormalities were noted on the autopsies, and as apparent from Fig. 3, the weights of the rats did not vary in the given time period. Rat 5 was still alive at 156 days post-implantation and has gained a substantial amount of weight.

### 3.2.2. Effect of TMZ delivery rate on efficacy

There were a total of 5 groups in this experiment: 9L control (tumor only), unactivated device (tumor + device), 1 membrane opened on day 0, 2 membranes open on day 0, and 3 membranes open on day 0. This experiment examines whether a faster rate of drug delivery, as opposed to a longer duration, results in increased median survival.

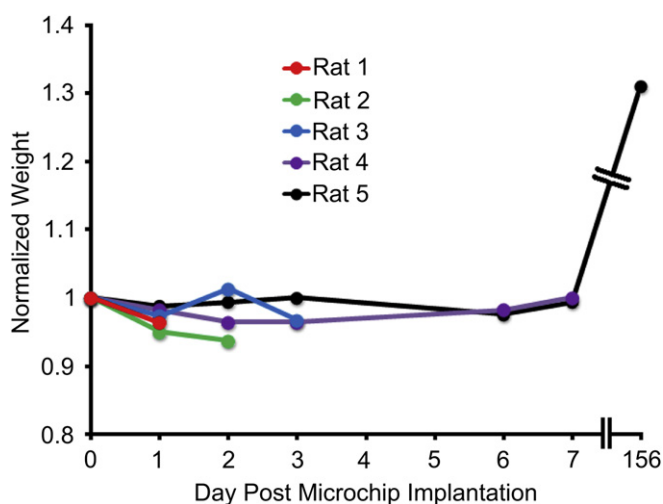


**Fig. 3.** Graphical presentation of normalized animal weight as a function of time. All animals displayed minimal weight loss during the acute phase, and animal 5 displayed robust weight gain over the chronic time scale.

The survival curves are depicted in Fig. 4A. Long term survivors are those animals surviving until the protocol mandated 120 day stop date. The no treatment controls and unactivated device groups had median survivals of 13 and 16 days, respectively (Table 1). The 3 membrane activated group had a median survival of 40 days with 42.8% long term survivors (LTS). The 2 membrane activated group had a median survival of 28 days and 28.5% LTS. The 1 membrane activated group had a median survival of 21 days with 12.5% LTS.

### 3.2.3. Effect of TMZ delivery time on efficacy

There were a total of 5 groups in this experiment: 9L control (tumor only), unactivated device (tumor + device), 3 membrane opened on day 0, 3 membranes open on day 3, and 3 membranes open on day 5. This experiment examines and quantifies the effect of earlier drug delivery.

The survival curves are depicted in Fig. 4B. Again, the no treatment controls and unactivated device groups had median survivals of 13 and 16 days, respectively (Table 1). The 3 membrane day 0 group had a median survival of 40 days with 42.8% LTS. The 3 membrane day 3 group had a median survival of 24 days and 12.5% LTS. The 3 membrane day 5 group had a median survival of 23 days and no LTS.

### 3.2.4. Comparison of the device to a polymer-based delivery system

Lastly, the efficacy of microchip-based delivery is compared with polymer-based drug delivery. There were a total of 5 groups in this experiment: 9L control (tumor only), unactivated device (tumor + device), 3 membranes opened on day 5, and 2 TMZ polymer-based wafers implanted on day 5. Both the device and the wafers contain 10 mg of TMZ and started to release drug on the same day.

The survival curves are depicted in Fig. 5B. Again, the no treatment controls and unactivated device groups had median survivals of 13 and 16 days, respectively (Table 1). The 3 membrane day 5 group had a median survival of 23 days and no LTS, and the 2 TMZ wafer group had a median survival of 34 days and LTS (Fig. 6).

## 3.3. Immunohistological analyses

Tissue samples were collected from animals that expired at or near the median survival date of that group. All treatment groups have elevated levels of cleaved Caspase-3 positive cells with the longest surviving group, 3 membranes activated on day 0, showing the second highest numbers of positive cells (Fig. 6A). The two longest surviving groups, 3 membrane day 0 and 2 TMZ wafer groups, have the fewest number Ki67 positive cells (Fig. 6B).

## 4. Discussion

Previous studies using the MEMS device had been restricted to rodent flank tumor models, due to large structural components. The adoption of injection molding technology, solid drug loading, and a redesign of the device geometry allowed for an 80 percent reduction in device volume for the same payload [29]. This is the first study to successfully demonstrate the efficacy of an active, intracranial microchip-based drug delivery system.

### 4.1. Function in vitro

*In vitro* release studies verified the reliable function of the active device. There are three criteria for 'reliable function.' First, TMZ release should occur only when the device has been activated. The leak test devices satisfied this criterion by remaining robustly sealed over the full time scale of the release study. It is important to note that all of the membranes remained intact in these devices



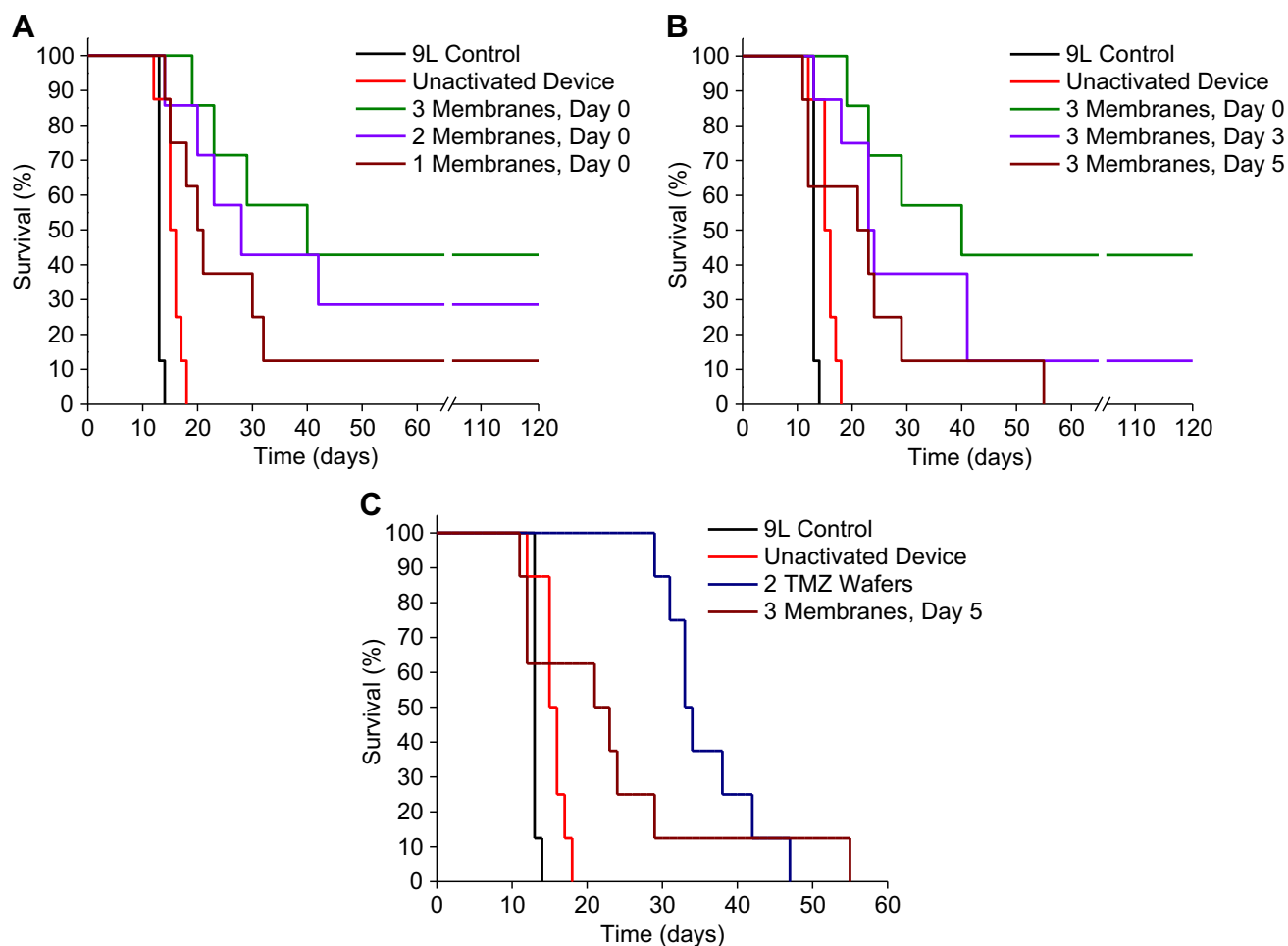


**Fig. 4.** Kaplan Meier survival curves. Animals receiving no treatment or unactivated devices had a median survival of 13 and 16 days respectively. (A) Impact of drug release rate on survival. Animals that received activated devices on day 0 had median survivals of 40 (42.8% LTS), 28 (28.5% LTS), and 21 (12.5% LTS) days for 3, 2, and 1 membranes activated respectively. (B) Impact of drug release time on survival. Animals that had all 3 membranes activated day 0, 3, or 5 had median survivals of 40 (42.8% LTS), 24 (12.5% LTS) and 23 days. (C) Comparison between microchip and polymer-based delivery methods. Those animals that received two TMZ:polymer wafers on day 5 had a median survival of 34 days, while those that had all 3 membranes opened on day 5 had median survival of 23 days.

and that the eventual leaking of these devices, therefore, reflects a degradation and failure of the sealing epoxy. Second, the rate of TMZ release should vary with the number of activated membranes. The release curves presented in Fig. 2 demonstrate that TMZ release rate is indeed a function of the number of membranes that have been activated and that a broad range of release rates can be achieved. Third, the kinetics of release should be reproducible for each scenario of device activation. Devices from each group displayed reproducible average rates for release, and most importantly were very consistent in overall extent and duration of release.

**Table 1**  
Survival data for the *in vivo* efficacy studies.

Treatment condition	n	Median survival (days)	% Long term survivors (n)
No treatment	8	13	0
Unactivated device	8	16*	0
Two TMZ wafers	8	34*	0
3 Membranes activated, day 0	7	40*	42.8 (3)
2 Membranes activated	7	28*	28.5 (2)
1 Membrane activated	8	21*	12.5 (1)
3 Membranes activated, day 3	8	24*	12.5 (1)
3 Membranes activated, day 5	8	23	0

\* $p < 0.05$  when compared to no treatment control.

#### 4.2. Preliminary *in vivo* studies

The device was demonstrated to be robust enough to survive the implantation procedure and remain in the animal long term. The electrical resistance across the fuses was measured after implantation and verified that the fuses were intact. It was also verified that fuse activation *in vivo* neither adversely or beneficially affects the survival of animals simultaneously implanted with a tumor (results not shown). The active device therefore can be used *in vivo* without diminishing the precise control over the timing of TMZ release or introducing competing effects in the analysis of survival in disease studies.

#### 4.3. Efficacy studies

The objective of this study was to determine the efficacy of TMZ delivered from the active device under different conditions. All treatment groups except the 3 membrane, day 5 group had significantly improved survival over the no treatment controls ( $p < 0.05$ , Table 1). The over-arching objective of designing a MEMS based active device capable of intracranial implantation and efficacy in rodent gliosarcoma model was achieved. The ability to activate different numbers of membranes at different times leads to some interesting insights into the function of this device and how disease progression may be deterred.

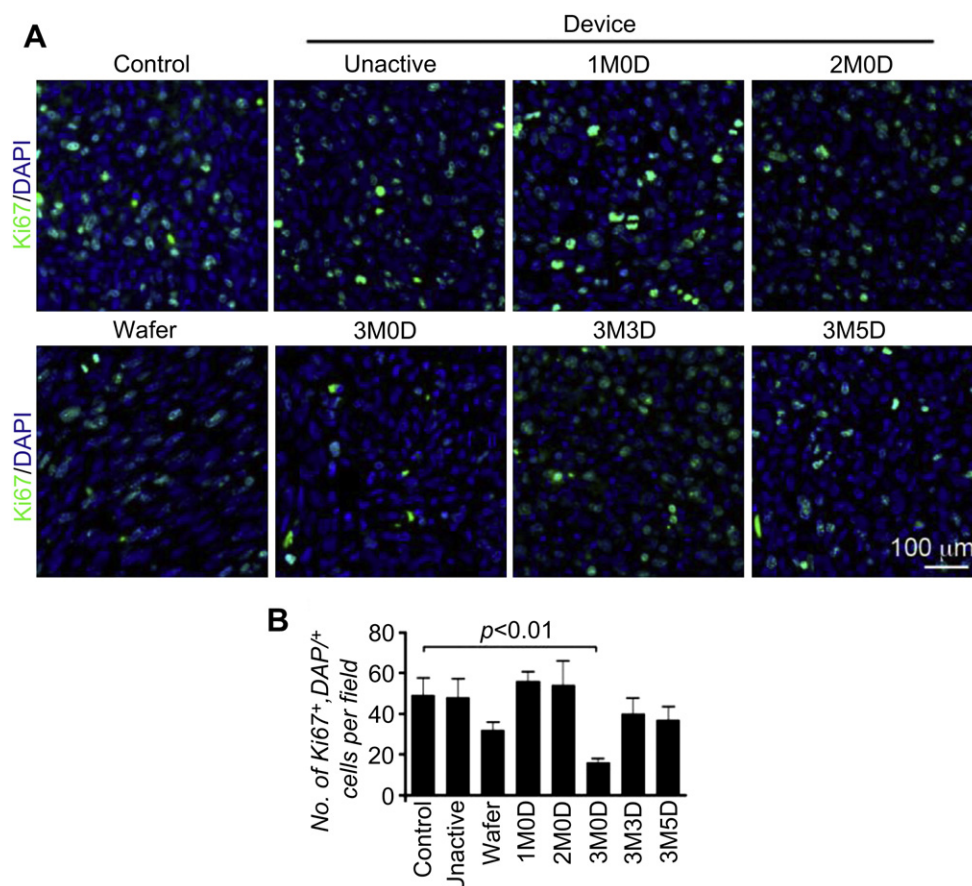


**Fig. 5.** Immunohistological results of Ki67 staining. (A) Ki67 positive cells are green and cell nuclei are blue. Each panel is a representative image from each efficacy study group. The 3M0D (3 membranes activated on day 0) panel contains the fewest number of Ki67 positive cells. (B) Quantitative results obtained by averaging 3 representative images from each group. The two longest surviving groups, wafer and 3M0D, have the lowest levels of Ki67 positive cells.

#### 4.3.1. Delivery rate

Each treatment group activated on day 0 had improved animal survival over the no treatment control. The  $p$  value when each day 0 treatment group is compared head to head is greater than 0.05, but there are 3 strongly indicative trends in the survival data that imply that a dose dependent type response is present within the day 0 groups. The survival curves (Fig. 4A) are all nested in order of device release rate with minimal overlap. The median survival of each group also trends with release rate. The day 0 groups have median survivals of 44, 28 and 21 days for 3, 2 and 1 membranes activated respectively. Finally, the percentage of long term survivors increases with the number of activated membranes (1 membrane: 12.5 %LTS, 2 membranes: 28.5 %LTS, 3 membranes: 42.8% LTS). These three trends when considered together indicate that rapid release, as opposed to longer duration, is more effective at retarding disease progression in this model.

#### 4.3.2. Delivery time

Head to head comparisons within the 3 membrane activated groups, again yields  $p$  values of greater 0.05, but similar trends emerge with date of activation as with number of activated membranes. The survival curves (Fig. 4B) are nested in order of activation date with groups receiving earlier activation faring better. Both median survival and the number of long term survivors increase with earlier activation: Day 5: 23 days, 0% LTS, Day 3; 24 days, 12.5% LTS, Day 0; 40 days, 42.8% LTS.

The decrease in median survival and long term survivors with delayed activation can be explained by two basic arguments

concerning tumor growth and device function. The longer the delay between tumor implantation and the initiation of treatment the more time the tumor has to grow. The TMZ distribution achieved by the active device *in vivo* is biased towards the face of the device that contains the membranes. The tumor is not only growing larger, but as it grows away from, and around the device it can also grow out of the 'therapeutic reach' of the device. Portions of the tumor, therefore, would be left unaddressed and free to proliferate. The conclusion from this set of experiments is that releasing drug sooner results in better median survival. This conclusion is consistent with experiences in the clinic, where earlier detection and treatment results in better survival for many cancers.

#### 4.3.3. Comparison to polymer-based drug delivery

Both the 3 membrane day 5 group and the wafer group released the same amount of TMZ (10 mg). The wafer group, however, had a median survival of 34 days, while the 3 membrane day 5 group had median survival of 23 days. Similar to the reasoning presented in the previous section, the wafers likely achieved better median survival because they release drug isotropically, while the micro-chips release drug from only 1 of 6 surfaces.

#### 4.4. Immunohistological analyses

Immunohistological analysis was conducted on tissue samples from the efficacy study with markers for cleaved Caspase-3 (a marker for apoptosis) and Ki67 (a marker for proliferation) (Fig. 6). TMZ causes DNA adducts, arresting the replication process and

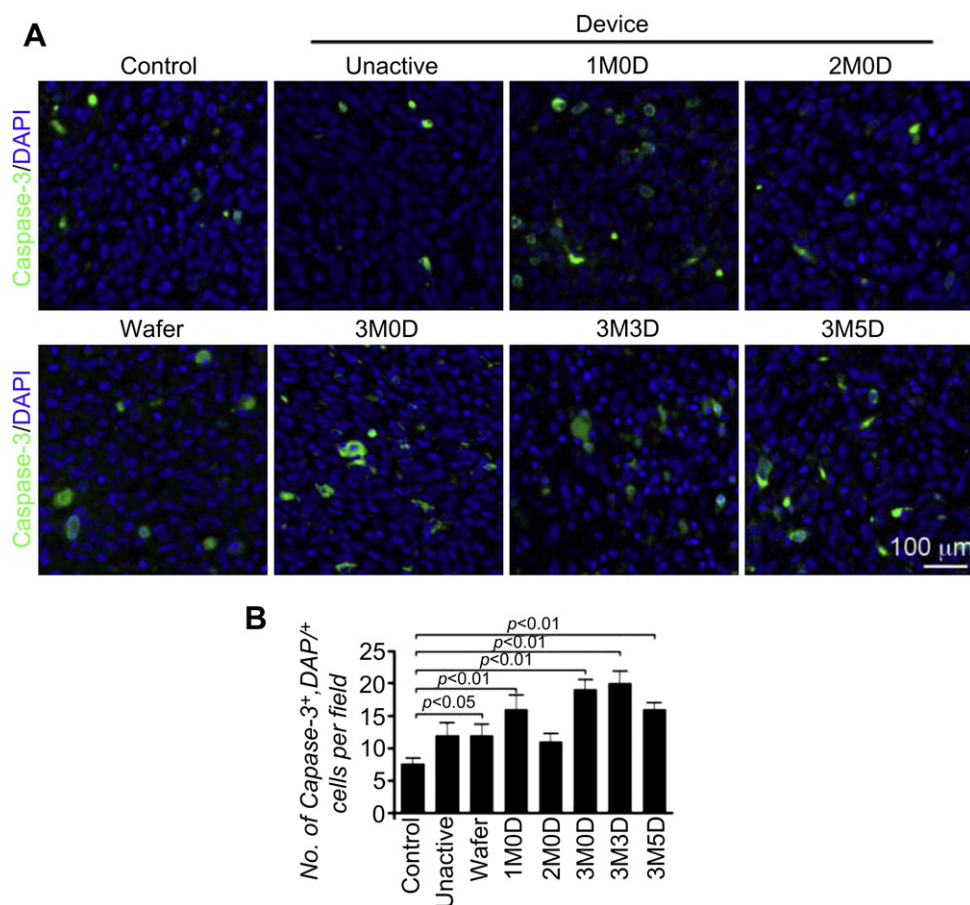


**Fig. 6.** Immunohistological results of Caspase-3 staining. (A) Caspase-3 positive cells are green and cell nuclei are blue. Each panel is a representative image from each efficacy study group. (B) Quantitative results obtained by averaging 3 representative images from each group. The 3M0D (3 membranes activated on day 0) panel contains the second highest number of caspase-3 positive cells.

initiating apoptosis [35]. Delivery of TMZ to a tumor mass should increase the number of cells undergoing apoptosis and commensurately reduce the number of actively proliferating cells, resulting in an increased number of cleaved Caspase-3 positive cells and reduced number of Ki67 positive cells. Animals receiving devices with 3 membranes activated on day 0 showed the second highest number of Caspase-3 positive cells, and lowest number of Ki67 positive cells (Fig. 6). This result confirms that TMZ is released in a viable, cytotoxic form, from the microchip device and is consistent with the results from the efficacy studies where the three membrane, day 0 group demonstrated the most prolonged survival.

## 5. Conclusions

A MEMS based depot drug delivery device capable of intracranial implantation in a rodent was developed in this work. The reliable and reproducible function of the device was confirmed *in vitro*. *In vivo* survival studies in a 9L gliosarcoma rodent study demonstrated that temozolomide delivery from the active device is capable of prolonging animal survival versus no treatment controls. The capabilities of this device introduce interesting opportunities for studying and understanding the interplay between drug delivery rate, the timing of release and disease progression. The ability to vary the release rate from the device with all other device properties remaining the same is an important tool for studies aimed at determining optimal release rates for certain drug:disease pairings. Delayed activation allows for studies to be conducted

where tumor and device are implanted simultaneously, but drug release is only initiated at a predetermined time sometime after implantation. This ability can be a powerful tool in studies where multiple therapeutics are to be delivered and the role of relative releasing timing is of interest (e.g. localized delivery of temozolomide and a potentiating factor such as O<sup>6</sup>-Benzylguanine). Implications of this work include the ability to implant a microchip containing a variety of drugs during intracranial tumor resection surgery. Based on the particular genetic abnormalities that develop, tailored combinations of drugs would be able to be locally delivered without the necessity of additional surgeries. We have shown the safety, kinetics, and efficacy of this method of drug delivery and compared it with one of the commonly implemented methods of intracranial drug delivery.

## Acknowledgments

This work was funded by the National Institute of Health (NIH Grant: EB006365). Y.X. is supported by the Swedish Research Council.

## References

- [1] Deorah S, Lynch CF, Sibenaller Z, Ryken TC. Trends in brain cancer incidence and survival in the United States: surveillance, epidemiology, and end results program, 1973 to 2001. *Neurosurg Focus* 2006;20(4):E1. 1–7.
- [2] Hou LC, Veeravagu A, Hsu AR, Tse VCK. Recurrent glioblastoma multiforme: a review of natural history and management options. *Neurosurg Focus* 2006; 20(4):E3. 1–9.

- [3] Stupp R, Mason WP, van den Bent MJ, Weller M, Fisher B, Taphoorn MJ, et al. Radiotherapy plus concomitant and adjuvant temozolomide for glioblastoma. *New Engl J Med* 2005;352(10):987–96.
- [4] Pardridge WM. Drug delivery to the brain. *J Cerebr Blood F Met* 1997;17(7):713–31.
- [5] Groothuis DR, Benalcázar H, Allen CV, Wise RM, Dills C, Dobrescu C, et al. Comparison of cytosine arabinoside delivery to rat brain by intravenous, intrathecal, intraventricular and intraparenchymal routes of administration. *Brain Res Int* 2000;856:281–90.
- [6] Lidar Z, Mardor Y, Jonas T, Pfeffer R, Faibel M, Nass D, et al. Convection-enhanced delivery of paclitaxel for the treatment of recurrent malignant glioma: a phase I/II clinical study. *J Neurosurg* 2004;100:472–9.
- [7] Sawyer AJ, Piepmeier JM, Saltzman WM. New methods for direct delivery of chemotherapy for treating brain tumors. *Yale J Biol Med* 2006;79:141–52.
- [8] Sampson JH, Akabani G, Friedman AH, Bigner D, Kunwar S, Berger M, et al. Comparison of intratumoral bolus injection and convection-enhanced delivery of radiolabeled antitenascin monoclonal antibodies. *Neurosurg Focus* 2006;20(4):E14. 1–4.
- [9] Raghavan R, Brady ML, Rodríguez-Ponce MI, Hartlep A, Pedain C, Sampson JH. Convection-enhanced delivery of therapeutics for brain disease, and its optimization. *Neurosurg Focus* 2006;20(4):E12.
- [10] Kawakami K, Kawakami M, Kioi M, Husain SR, Puri RK. Distribution kinetics of targeted cytotoxin in glioma by bolus or convection-enhanced delivery in a murine model. *J Neurosurg* 2004;101:1004–11.
- [11] Brem S, Tyler B, Li K, Pradilla G, Legnani F, Caplan J, et al. Local delivery of temozolomide by biodegradable polymers is superior to oral administration in a rodent glioma model. *Canc Chemother Pharmacol* 2007;60(5):643–50.
- [12] Guerin C, Olivi A, Weingart JD, Lawson HC, Brem H. Recent advances in brain tumor therapy: local intracerebral drug delivery by polymers. *Invest New Drug* 2004;22(1):27–37.
- [13] Tyler B, Fowers KD, Li KW, Recinos VR, Caplan JM, Hdeib A, et al. A thermal gel depot for local delivery of paclitaxel to treat experimental brain tumors in rats. *J Neurosurg* 2010;113(2):210–7.
- [14] Lesniak MS, Upadhyay U, Goodwin R, Tyler B, Brem H. Local delivery of doxorubicin for the treatment of malignant brain tumors in rats. *Anticancer Res* 2005;25(6B):3825–31.
- [15] Westphal M, Hilt DC, Bortey E, Delavault P, Olivares R, Warnke PC, et al. A phase 3 trial of local chemotherapy with biodegradable carmustine (BCNU) wafers (gliadel wafers) in patients with primary malignant glioma. *Neuro-oncol* 2003;5(2):79–88.
- [16] Valtanen S, Timonen U, Toivanen P, Kalimo H, Kivipelto L, Heiskanen O, et al. Interstitial chemotherapy with carmustine-loaded polymers for high-grade gliomas: a randomized double-blind study. *Neurosurgery* 1997;41(1):44–8. discussion 8–9.
- [17] Lesniak MS, Brem H. Targeted therapy for brain tumours. *Nat Rev Drug Discov* 2004;3(6):499–508.
- [18] McGirt MJ, Than KD, Weingart JD, Chaichana KL, Attenello FJ, Olivi A, et al. Gliadel (BCNU) wafer plus concomitant temozolomide therapy after primary resection of glioblastoma multiforme. *J Neurosurg* 2009;110(3):583–8.
- [19] Scott AW, Tyler BM, Masi BC, Upadhyay UM, Patta YR, Grossman R, et al. Intracranial microcapsule drug delivery device for the treatment of an experimental gliosarcoma model. *Biomaterials* 2011;32(10):2532–9.
- [20] Pradilla G, Wang PP, Gabikian P, Li K, Magee CA, Walter KA, et al. Local intracerebral administration of paclitaxel with the paclimer delivery system: toxicity study in a canine model. *J Neuro Oncol* 2006;76(2):131–8.
- [21] Maloney JM, Uhland SA, Polito BF, Sheppard Jr NF, Pelta CM, Santini JT. Electrothermally activated microchips for implantable drug delivery and biosensing. *J Control Release* 2005;109:244–55.
- [22] Prescott JH, Lipka S, Baldwin S, Sheppard Jr NF, Maloney JM, Coppeta J, et al. Chronic, programmed polypeptide delivery from an implanted, multireservoir microchip device. *Nat Biotechnol* 2006;24(4):437–8.
- [23] Santini JT, Cima MJ, Langer R. A controlled-release microchip. *Nat Biotechnol* 1999;397:335–8.
- [24] Santini JT, Richards AC, Scheidt R, Cima MJ, Langer R. Microchips as controlled drug-delivery devices. *Angew Chem Int Ed* 2000;39:2396–407.
- [25] Santini Jr JT, Richards AC, Scheidt RA, Cima MJ, Langer RS. Microchip technology in drug delivery. *Ann Med* 2000;32(6):377–9.
- [26] Elman NM, Lipka Y, Scott AW, Masi B, Ho Duc HL, Cima MJ. The next generation of drug-delivery microdevices. *Clin Pharmacol Ther* 2009;85(5):544–7.
- [27] Elman NM, Upadhyay UM. Medical applications of implantable drug delivery microdevices based on MEMS (micro-electro-mechanical-systems). *Curr Pharmaceut Biotechnol* 2010;11(4):398–403.
- [28] Cima MJ. Microsystem technologies for medical applications. *Annu Rev Chem Biomol Eng* 2011;2(1):355–78.
- [29] Li Y, Ho Duc HL, Tyler B, Williams T, Tupper M, Langer R, et al. In vivo delivery of BCNU from a MEMS device to a tumor model. *J Control Release* 2005;106:138–45.
- [30] Li Y, Shawgo RS, Tyler B, Henderson PT, Vogel JS, Rosenberg A, et al. In vivo release from a drug delivery MEMS device. *J Control Release* 2004;100:211–9.
- [31] Elman NM, Ho Duc HL, Cima MJ. An implantable MEMS drug delivery device for rapid delivery in ambulatory emergency care. *Biomed Microdevices* 2009;11(3):625–31.
- [32] Farra R, Sheppard Jr NF, McCabe L, Neer RM, Anderson JM, Santini Jr JT, et al. First-in-human testing of a wirelessly controlled drug delivery microchip. *Sci Transl Med* 2012;4(122):122ra21.
- [33] Kim HK, C-c Lin, Parker D, Veals J, Lim J, Likhari P, et al. High-performance liquid chromatographic determination and stability of 5-(3-methyltriazene-1-yl)-imidazo-4-carboximide, the biologically active products of the antitumor agent temozolomide, in human plasma. *J Chrom B* 1997;703:225–33.
- [34] Elman NM, Masi BC, Cima MJ, Langer R. Electro-thermally induced structural failure actuator (ETISFA) for implantable controlled drug delivery devices based on micro-electro-mechanical-systems. *Lab Chip* 2010;10(20):2796–804.
- [35] Newlands ES, Stevens MFG, Wedge SR, Wheelhouse RT, Brock C. Temozolomide: a review of its discovery, chemical properties, pre-clinical development and clinical trials. *Canc Treat Rev* 1997;23:35–61.
- [36] Xue Y, Lim S, Yang Y, Wang Z, Jensen LD, Hedlund EM, et al. PDGF-BB modulates hematopoiesis and tumor angiogenesis by inducing erythropoietin production in stromal cells. *Nat Med* 2011;18(1):100–10.